Hydrated and Dehydrated Tertiary Interactions–Opening and Closing–of a Four-Helix Bundle Peptide

Martin Lignell,[†] Lotta T. Tegler,[‡] and Hans-Christian Becker[†*]
[†]Department of Photochemistry and Molecular Sciences, and [‡]Department of Biochemistry and Organic Chemistry, Uppsala University, Uppsala, Sweden

ABSTRACT The structural heterogeneity and thermal denaturation of a dansyl-labeled four-helix bundle homodimeric peptide was studied with steady-state and time-resolved fluorescence spectroscopy and with circular dichroism (CD). At room temperature the fluorescence decay of the polarity-sensitive dansyl, located in the hydrophobic core region, can be described by a broad distribution of fluorescence lifetimes, reflecting the heterogeneous microenvironment. However, the lifetime distribution is nearly bimodal, which we ascribe to the presence of two major conformational subgroups. Since the fluorescence lifetime reflects the water content of the four-helix bundle conformations, we can use the lifetime analysis to monitor the change in hydration state of the hydrophobic core of the four-helix bundle. Increasing the temperature from 9°C to 23°C leads to an increased population of molten-globule-like conformations with a less ordered helical backbone structure. The fluorescence emission maximum remains constant in this temperature interval, and the hydrophobic core is not strongly affected. Above 30°C the structural dynamics involve transient openings of the four-helix bundle structure, as evidenced by the emergence of a water-quenched component and less negative CD. Above 60°C the homodimer starts to dissociate, as shown by the increasing loss of CD and narrow, short-lived fluorescence lifetime distributions.

INTRODUCTION

Conformational dynamics (1) is an important factor in the function (2,3), folding (4–6), and recognition of proteins (7–9). Understanding the underlying mechanisms that govern polypeptide dynamics is therefore of fundamental interest. Conformational changes are known to take place on different timescales (4,10) and involve changes in the surrounding water as well (11–17).

A number of experimental techniques, such as NMR (18,19), Förster resonance energy transfer (FRET), single-molecule spectroscopy, and time-resolved fluorescence/optical spectroscopy have been used to probe the conformational dynamics of proteins (20–28). A distinct advantage of optical spectroscopy methods is their ability to measure dynamical processes on the nanosecond timescale and faster. The disadvantage of such methods is their lack of atomic resolution; however, conformational diversity can be extracted from the distribution of the fluorescence lifetimes of intrinsic fluorophores (29). In this work we report the temperature dependence of the fluorescence lifetime distribution of dansyl inside a four-helix bundle peptide. Since the fluorescence lifetime varies with the bulk polarity of the solvent, we believe that the fluorescence lifetime also reflects the water content near the fluorophore.

Several studies of conformational dynamics have been done with single-molecule spectroscopy and FRET. The conformational transitions of the helical proteins apomyoglobin (30–34) and syntaxin-1 (35) have been shown to take place on the microsecond to millisecond timescale. One question related to the dynamics concerns which structural changes are involved in the conformational transitions. The structural fluctuations observed in apomyoglobin increase with increasing molten globule character of the protein. Judging from this, the conformational dynamics observed in apomyoglobin may be transitions between the native state and the molten globule state.

Using optical tweezers in a dynamical study of the RNase protein, Cecconi et al. (6) showed that the single RNase molecule continuously switched between an intermediate and compact extended state when the optical tweezers were loaded with a certain force. They concluded that the RNase molecule switched between the native and the molten-globule state.

In previous kinetic protein refolding experiments, intermediates were identified in apomyoglobin (36–38) and cytochrome *c* (39). By following the amide I′ vibrational state in time, Nishiguchi et al. (36) were able to observe that solvated helices preceded buried helices. The preceding solvated state was considered to be as compact as the final native state. As the protein moves toward the native state, desolvation accompanies the formation of a globular structure. The transition from the compact water-containing state to the dehydrated native state is kinetically limited by enthalpic barriers connected to the desolvation process (40). However, desolvation is entropically favored, and this can result in a low net free-energy barrier (13). In general, based on these observations, it is believed that in many cases the equilibrium dynamics of polypeptides correspond to transitions between hydrated and nonhydrated states of the polypeptide.

To test this idea, it would be necessary to probe structural fluctuations in a region of a polypeptide that can be in either a folded or partly unfolded state. The hydrophobic core of a

Submitted October 16, 2008, and accepted for publication April 1, 2009.

*Correspondence: hcb@fotomol.uu.se

Editor: Alberto Diaspro.

0006-3495/09/07/0572/9 $2.00

doi: 10.1016/j.bpj.2009.04.055

four-helix bundle consists of packed hydrophobic side chains from different helices that, at least hypothetically, could be in contact with water if the bundle is not in its most closely packed form. In this work, we studied a four-helix bundle peptide using time-resolved fluorescence spectroscopy (TCSPC). The homodimeric four-helix bundle carries two fluorophores (both of which are dansyl) covalently attached to the side chain of a lysine residue in the middle of the helix (41). We show that dansyl works as a probe of the tertiary structure of the four-helix bundle peptide, utilizing the fact that the fluorescence lifetime as well as emission wavelength of dansyl is sensitive to the polarity of the microenvironment.

By analyzing the fluorescence decay with a maximal distribution of lifetimes (maximum entropy), we find two different groups of lifetimes. The subdistribution with the longest lifetimes represents conformations that have a fully developed hydrophobic core. The other group has shorter lifetimes, but these are still much longer than the lifetime of dansyl in water, showing that the dansyls in this group are at least partially protected from water. Maximum entropy analysis of the fluorescence lifetimes yields fairly broad distributions. Given the sensitivity of the dansyl emission lifetime to polarity, we interpret this as significant heterogeneity inside the hydrophobic core. Even though the intrinsic polarity of the peptide (42,43) affects the lifetime of the dansyl, because of its much higher dielectric constant, the effects on the dansyl lifetime from increased water accessibility to the hydrophobic core are expected to be much stronger than those from the peptide matrix.

MATERIALS AND METHODS

Materials

The four-helix bundle peptide, $(KE2\text{-}D15)_2$, is a de novo design structure that in solution forms an antiparallel homodimer comprising two helix-loop-helix monomers. Dimerization into a four-helix bundle occurs with high affinity ($K_D < 10\ \mu M$, estimated from the red shift in emission wavelength with dilution), mainly through hydrophobic interactions (41). The amino acid sequence of the monomer (Fig. 1) is based on a repeat heptad pattern in which the first and fourth amino acids form the hydrophobic core. Residues 2 and 5 control dimerization, and residues 3 and 7 in the heptad are on the solvent-exposed side of the four-helix bundle. Although the exact structure of the peptide dimer is not known, circular dichroism (CD) measurements and analytical ultracentrifugation and NMR data have provided conclusive evidence of a four-helix bundle structure (44,45). In this study, the polarity probe dansyl was introduced on residue 15 (lysine). Structural changes in the hydrophobic region should thus be reflected in changes in the emission spectrum and the fluorescence lifetime of dansyl. See the Supporting Material for details on the procedures used for synthesis and purification.

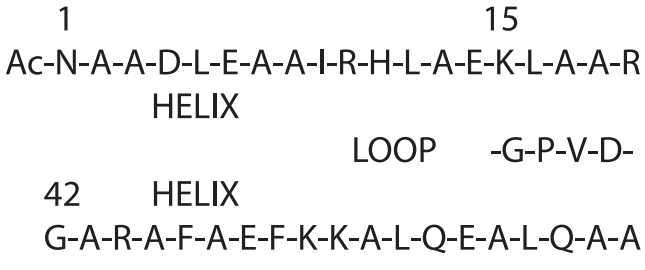

FIGURE 1 Amino acid sequence of the helix-loop-helix monomer KE2. Dansyl is attached to the side chain of lysine 15.

The lyophilized oligopeptide was reconstituted in 100 mM sodium phosphate buffer (pH 7.20). Steady-state fluorescence, TCSPC, and CD measurements were obtained from solutions containing 100 μM KE2-D15 monomer. Under these conditions, >95% of the peptide is present as dimer at room temperature (see above).

As a reference for dansyl emission in environments of different polarities, dansylglycine (Sigma-Aldrich, Stockholm, Sweden) was used without further purification. The emission spectra and fluorescence lifetimes of dansylglycine were measured in water, methanol, and ethanol.

Equilibrium measurements of the $(KE2\text{-}D15)_2$ structure were performed between 9°C and 80°C.

Methods

Steady-state emission spectra of native and denatured $(KE2\text{-}D15)_2$, as well as those of dansylglycine, were recorded with SPEX Fluorolog-2 and Fluorolog-3 double-monochromator fluorimeters. All spectra were corrected for the wavelength-dependent transmission of the emission monochromator and the wavelength-dependent sensitivity of the detector PMT. Spectral bandwidths were 5 nm for both excitation and emission monochromators. The dansyl chromophore has an absorption band centered at 335 nm, and the location and intensity of this band are practically independent of solvent polarity. By contrast, the emission maximum is strongly dependent on the environment. Fluorescence spectra of the peptide were recorded in a 3 × 3 mm reduced cuvette. The optical density at 335 nm was ≈0.1 for 100 μM KE2-D15. To determine the emission maximum wavelength more accurately, emission maxima were found by calculating the center of gravity in the corrected emission spectra using the following equation:

$$\lambda_{\text{center of gravity}} = \frac{\sum_i \lambda_i \times I(\lambda_i)}{\sum_i I(\lambda_i)}. \quad (1)$$

The CD spectra of the peptide bond absorption region were recorded between 190 and 250 nm on the native and denatured $(KE2\text{-}D15)_2$ using a Jasco J-810 spectrometer and a spectral bandwidth of 1 nm. The CD at 220 nm was used to quantify the α-helix content at different temperatures.

Fluorescence lifetime measurements of dansyl were obtained by means of a time-correlated single-photon counting system as described previously (46). Briefly, the frequency-doubled output of a Coherent RegA-900 was used to produce 670 nm light in a Coherent OPA-9000 optical parametric amplifier. The output from the OPA was frequency-doubled in a BBO crystal to produce 100 fs, 335 nm pulses. Excitation light was polarized vertically, and the emission was taken through a polarizer set to the magic angle condition. Fluorescence was detected using a Hamamatsu MCP. The full-width at half maximum of the instrument response function was typically 50 ps. The fluorescence decays were recorded close to the uncorrected emission maximum at 560 nm using 10 nm bandpass filters.

Decays at 560 nm were fitted using a maximum-entropy algorithm for dansylglycine in solvents, and for dansyl from the four-helix bundle. The maximum-entropy algorithm was implemented in MATLAB (The MathWorks, Natick, MA), following the theory of Vinogradov and Wilson (47). The fluorescence decay is assumed to consist of a distribution of lifetimes according to Eq. 2, and the data analysis extracts the probability distribution $P(\tau)$ of time constants that describes the fluorescence decay $Y(t)$. All time constants were initially chosen to be equally probable in the interval $10^{-2} < t < 10^{2}$ ns with a factor of $10^{0.01}$ ns between consecutive time constants. The goodness of fit was determined by a χ^2 test, and in all cases χ^2 was below 1.10.

$$Y(t) = \int_{0.01}^{100} P(\tau) \times \exp(-t/\tau) d\tau \qquad (2)$$

RESULTS

For dansyl, the emission wavelength (Fig. 2 *a*) and fluorescence lifetime (Fig. 2 *b*) change with the bulk polarity of the solvent. The center of gravity (Eq. 1) of the dansyl emission is 613 nm in water ($\varepsilon = 80$), 573 nm in methanol ($\varepsilon = 32.7$), and 567 nm in ethanol ($\varepsilon = 24.3$). Fig. 2 *b* shows the distributions of fluorescence lifetimes in dansyl in the corresponding solvents. As expected for a fluorophore in a homogeneous solvent, the fluorescence lifetime distributions of dansyl in the different solvents are very narrow, in stark contrast to the broad distribution of lifetimes found for the four-helix bundle peptide $(KE2\text{-}D15)_2$, shown in Fig. 3 *a* (the distribution at room temperature). The fluorescence lifetime of dansyl is 2.4 ns in water, 11.4 ns in methanol, and 12.8 ns in ethanol. These time constants, taken from the maximum entropy distributions (Fig. 2 *b*), also correspond to the single time constant obtained from fitting the data to a single exponential decay (data not shown). Thus, the width of the peak in the maximum entropy analysis is that expected for a single-exponential decay, and the lifetime distributions obtained for the peptide are compared with this width. The changes in the emission wavelength and fluorescence lifetime of dansyl with the bulk polarity of solvents show that dansyl fluorescence can be used to probe the polarity of microenvironments. Of importance, the emission lifetime of dansylglycine is practically independent of temperature (Fig. 3 *b*), which enables us to attribute the observed variations in the fluorescence lifetimes in the peptide to structural changes in the four-helix bundle structure when the temperature is raised, rather than to changes in the intrisic photophysics of the dansyl.

The CD spectrum in Fig. 4 *a* shows negative differential absorption at 220 nm, which indicates that the KE2-D15 oligopeptide dimer has helical structure. Fig. 4 *b* shows the steady-state emission spectrum of the KE2-D15 dimer. The center of gravity wavelength of the emission spectrum at room temperature is 567 nm. Based on the solvent dependence of the dansyl emission, this corresponds to a nonpolar time-averaged microenvironment around the two dansyl fluorophores, and from this we assign them to mainly be in the hydrophobic core region of the dimer.

Fluorescence lifetime distribution at low temperatures

The fluorescence lifetime distribution of dansyl in the four-helix bundle peptide Fig. 3 *a* (the distribution at room temperature) is much broader than the lifetime distribution of dansylglycine in water and organic solvents (Fig. 2 *b*). In fact, the fluorescence lifetime distribution of the four-helix bundle is composed of three subdistributions. The subdistributions have their maximum probabilities at 4.2 ns, 9.9 ns, and 20.2 ns, respectively. We now consider the question as to why the fluorescence decay of dansyl in the four-helix bundle (Fig. 5 *a*) is so complex relative to the decay in water (Fig. 5 *b*) or any other solvent. The maximum entropy analysis works well for both decays with a χ^2-value of 1.05 and 1.06 for dansylglycine in water and dansyl in the four-helix bundle, respectively. Since the dansyl fluorophore is connected to lysine 15, which is part of the hydrophobic core, the structural changes likely associated with fluctuations in the hydrophobic core occur on a timescale slower than the nanosecond timescale for the fluorescence decay (10,30). If the conformational changes were occurring on a subnanosecond time scale, we would not see separate distributions of lifetimes.

The fluorescence lifetime distributions in Fig. 3 *a* (the distribution at room temperature) show a large variation in the probability of time constants. The presence of subdistributions indicates that the structural features in the three groups are related to different polarities in the hydrophobic core, as the emission lifetime of dansyl depends on the polarity of the microenvironment (50). These differences in polarities can be due to different degrees of hydration of

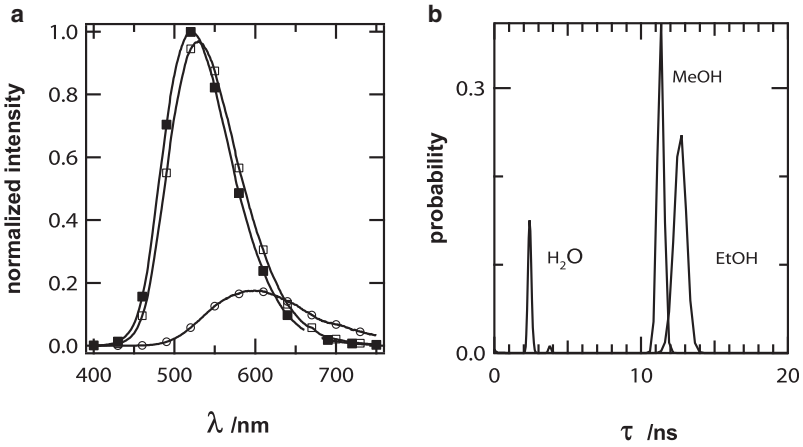

FIGURE 2 (*a*) Emission spectra of dansylglycine in water (*open circles*), methanol (*open boxes*), and ethanol (*solid boxes*). The emission intensity is normalized to that in the least-polar solvent (ethanol). Increasing polarity leads to decreasing emission intensity because of the decreasing fluorescence lifetime and quantum yield. The peak at 670 nm is twice the excitation wavelength (335 nm) and is an artifact from the emission monochromator. (*b*) Probability distributions of fluorescence lifetimes of dansylglycine in water, methanol, and ethanol.

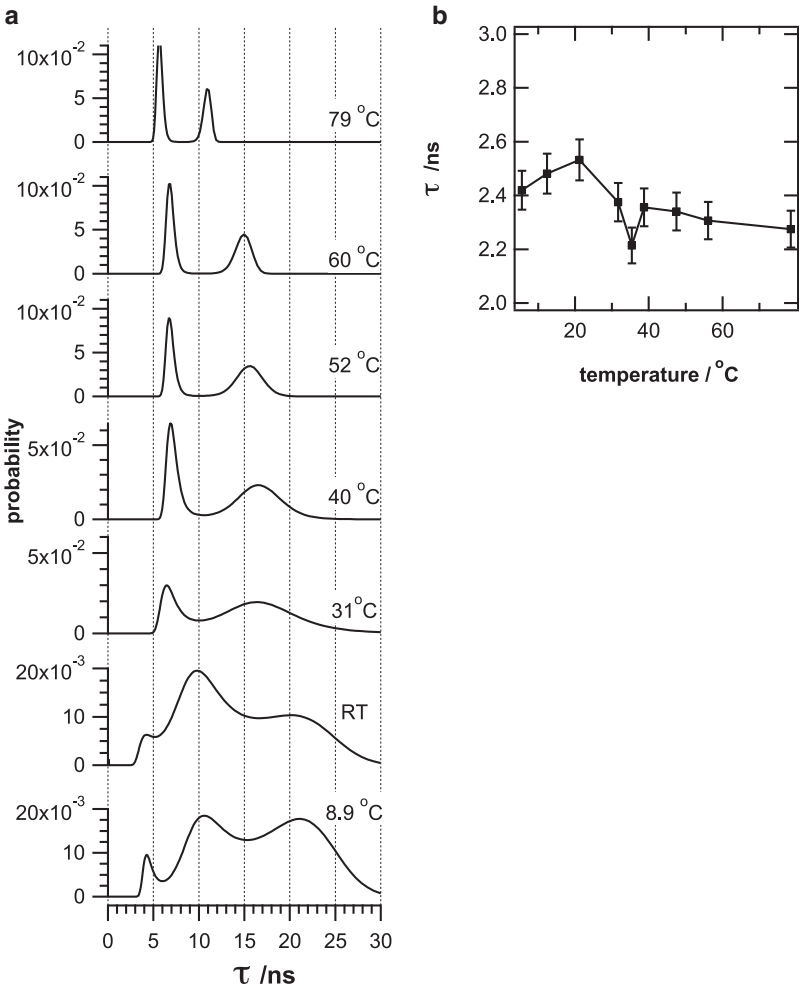

FIGURE 3 (*a*) Probability distributions of fluorescence lifetimes of the four-helix bundle at 8.9, 23, 31, 40, 52, 60, and 79°C. (*b*) Fluorescence lifetime of dansylglycine in H_2O as a function of temperature.

the hydrophobic core (51). In contrast to polarity effects, other quenching mechanisms can reduce the lifetime of dansyl without giving the concurrent red shift of the emission that results from increased polarity.

The distribution centered around the 4.2 ns lifetime of the first group is fairly close to the fluorescence lifetime of dansylglycine in water (2.4 ns). This lifetime comes out as a well separated, narrow distribution at the lowest temperature (8.9°C). Increasing temperature broadens the distribution, and above 31°C the component disappears completely (Fig. 3 *a*). Low temperatures (10–25°C) are expected to stabilize and enhance protein structure in general, which suggests that the quenching mechanism resulting in the 4.2 ns time constant likely originates in some specific interaction, such as electron transfer quenching from a nearby residue, and not from hydration of this specific molecular environment. We note that if the short component were a result of hydration, we would observe a blue shift (toward lower

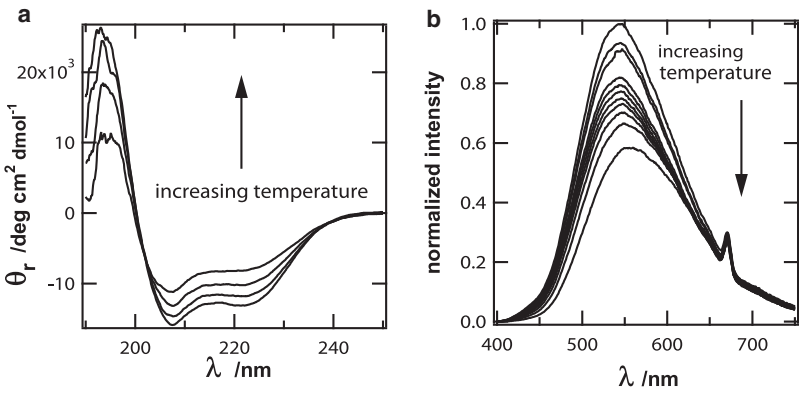

FIGURE 4 (*a*) CD spectra of the four-helix bundle $(KE2D\text{-}15)_2$, starting from the bottom, at 20, 40, 60, and 80°C. The absolute error in the CD magnitude is estimated to be <10%, and the error between measurements is $<50^\circ \times cm^2 \times dmol^{-1}$. (*b*) Dansyl emission spectra of $(KE2\text{-}D15)_2$ for excitation at 335 nm, starting from the top, at 11, 16, 26, 32, 35, 39, 44, 49, 58, 68, and 81°C. The peak at 670 nm is due to the emission monochromator transmitting $2 \times \lambda_{exc}$.

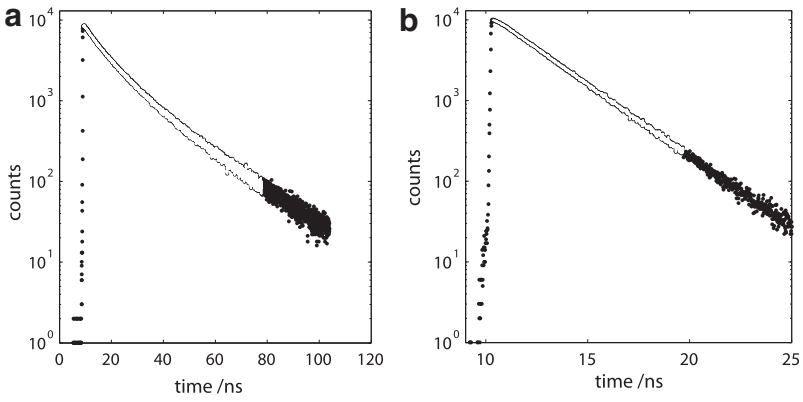

FIGURE 5 (*a*) Decay of dansyl in the four-helix bundle $(KE2\text{-}D15)_2$. (*b*) Decay of dansylglycine in H_2O. The fluorescence decay is displayed in black points, and the maximum-entropy distribution fit $Y(t)$ (Eq. 1) is overlaid in white. The fitting region included all channels with more than 100 counts (standard deviation $< 10\%$).

polarity) of the steady-state emission spectrum with decreasing temperature—something our data do not show.

Given the behavior of the steady-state emission, in conjunction with the temperature-dependent CD spectra (see below), we attribute the time constants in the second and third groups to different polarities around the dansyls. The CD and emission spectra show that the polypeptide dimer has helical structure and that dansyl is buried in the hydrophobic core. The second and third groups have maximum probable time constants at 9.9 ns and 20.2 ns, respectively (Table 1). We believe the bimodal distribution of long lifetimes is due to the presence of a hydrated hydrophobic core along with a dehydrated hydrophobic core of the four-helix bundle. Our reasoning is as follows: a fluorescence lifetime of 9.9 ns is comparable to the lifetime of dansylglycine in a solvent of intermediate polarity ($\varepsilon \approx 30$), whereas a lifetime of 20.2 ns corresponds to a folded, shielded environment with low polarity (42,43,50). These two types of hydrated and dehydrated hydrophobic core structures are present at the same time in the ensemble of four-helix bundle peptides, and each four-helix bundle molecule changes its hydration state on a slower timescale than the nanosecond fluorescence (10,30). We thus assign components 2 and 3 in the distribution to structures in which the hydrophobic core is partially or fully dehydrated, respectively.

TABLE 1 Approximate area of the three subdistributions (A_1, A_2, and A_3) of fluorescence lifetimes as a percentage of the total distribution, and maximal probable lifetime of each subdistribution at different temperatures

Temperature (°C)	A_1	A_2	A_3	τ_1 (ns)	τ_2 (ns)	τ_3 (ns)
8.9	5	37	58	4.2	10.6	21.2
23	5	59	36	4.2	9.9	20.2
30.9	0	27	73	0	6.4	16.4
40.3	0	42	58	0	6.8	16.4
51.7	0	45	55	0	6.7	15.7
59.7	0	52	48	0	6.8	15
79.0	0	60	40	0	5.7	10.9

Areas are calculated by integration from the minimum in the trough before the peak to the minimum after the peak. Uncertainties in areas are $\pm 3\%$. Peak lifetimes are $\pm 5\%$.

Effects of increased temperature

Temperature affects the distribution of four-helix bundle conformations strongly, as shown by the change in the appearance of the distributions of lifetimes in Fig. 3 *a*. We can see two different modes of conformational equilibria between the four-helix bundle conformations. The distribution of fluorescence lifetimes at 8.9°C and at room temperature differs significantly from that at 31°C and higher temperatures. The peak of the longest time constants has shifted from $\approx$20 ns at room temperature to $\approx$16 ns at 31°C (Table 1 and Fig. 3 *a*). In parallel, the peak of the intermediate time constants has shifted from $\approx$10 ns at room temperature to $\approx$6 ns at 31°C, and, as noted above, the sharp peak around 4 ns has disappeared. The reduction of fluorescence lifetimes is a spectroscopic signature indicating that the four-helix bundle is becoming more flexible, thus admitting more water into the core at temperatures above 31°C. Thus, this represents a gradual hydration of the four-helix bundle structure, causing an increase in polarity in the environment proximate to dansyl. However, the presence of the 16 ns component indicates that some dansyls still experience a relatively nonpolar environment, in line with the presence of tertiary interactions between the two KE2-D15 monomers. Most likely, this conformation is another type of four-helix bundle structure that contains more water than the conformation represented by the 20 ns component at room temperature.

Structural changes at high temperatures

Judging from the decrease in width of the 6–7 ns peak at $\geq$40°C, the structures that give rise to this group of time constants in all likelihood do not represent a proper four-helix bundle structure. We base this on the short lifetime, which indicates a polar environment, and the narrow width, which indicates little heterogeneity in the polarity sensed by the dansyl, both of which are in agreement with the dansyl being unable to avoid water by inserting itself into a hydrophobic core. Moreover, the most unstructured and solvated KE2-D15 polypeptide conformation, which we should observe at the highest temperature (79°C), gives a similar most probable lifetime (5.7 ns; Table 1). The fraction of

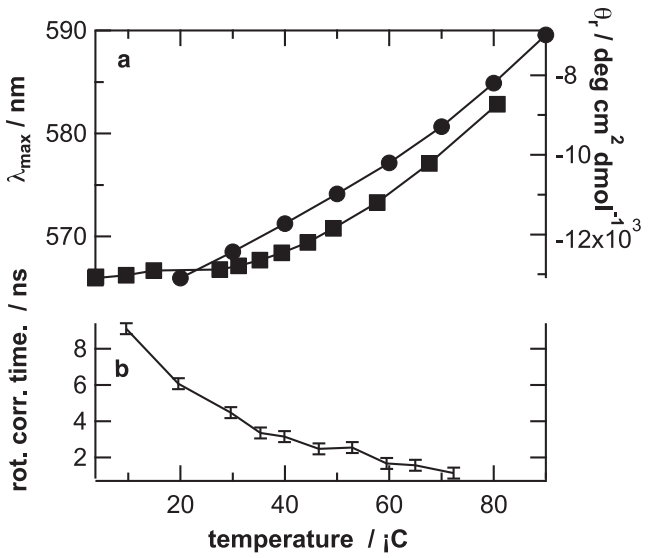

FIGURE 6 (*a*) Emission center of gravity wavelength (*solid boxes*; uncertainty ±0.1 nm) and mean residue ellipticity at 220 nm of KE2-D15 (*solid circles*) as a function of temperature. (*b*) Measured rotational correlation time (from time-resolved fluorescence anisotropy) of dansyl in the KE2-D15 four-helix bundle peptide between 10°C and 72°C.

the second group of time constants also increases, from 27% at 31°C to 60% at 79°C.

The onset of structural changes of the four-helix bundle at ~30°C is also evident by a red shift of the emission maximum of dansyl. The emission maximum increases monotonously after 31°C, but is almost constant at 567 nm below that temperature (Fig. 6 *a*). This increase in the emission maximum, corresponding to an on-average more polar environment for the dansyl, is another sign of dissociation or opening of the $(KE2\text{-}D15)_2$ homodimer above 31°C. The temperature threshold is also borne out in reversibility experiments, where we observe some loss of peptide fluorescence (~20%), presumably through precipitation, when solutions are heated above 30–35°C and subsequently slowly cooled to room temperature. Cooling from 80°C to room temperature recovers a slightly more red-shifted spectrum (data not shown), not the initial emission maximum wavelength, suggesting that refolding from a thermally denatured state does not occur in the fully native state.

Effect of temperature on CD and possible dissociation of the dimer

The overall helical content of the ensemble of four-helix bundles, measured as the negative mean residue ellipticity at 220 nm, decreases slightly and monotonously with increasing temperature (Fig. 6 *a*). Less ordered organization of the backbone seems to correlate with increased hydration of the four-helix bundle conformations.

Even at high temperatures (79°C) there is a significant amount of helicity in the structures, as seen from the negative CD (Fig. 6 *a*). Thus we have situation in which the emission maximum of the dansyl fluorescence indicates that the peptide is in a highly hydrated state, and quite possibly dissociated into monomers, but the CD shows an at least partly helical backbone. With our spectroscopic methods, we cannot distinguish between monomeric KE2-D15 and a highly disordered dimer. However, we note that dimer formation likely stabilizes the helical structure of the peptide, and the presence of a significantly negative mean residue ellipticity at 220 nm at 79°C could mean that even under such harsh conditions a sizeable amount of dimers may be present.

DISCUSSION

Interpretation of the fluorescence lifetimes

Before discussing the results, we would like to point out that all of the measurements in this study were obtained from systems in equilibrium. Furthermore, the timescale for the large-scale conformational transitions we will be discussing is longer than that of the fluorescence decays (10). This means that we can determine the conformational heterogeneity through the heterogeneity of the fluorescence decay because the different conformations essentially represent different photophysical species. There will certainly be some degree of rapid local motion in both well-packed and unfolded structures. Just as with exchange processes in NMR spectroscopy, the timescale for that local motion relative to that of the fluorescence lifetime can result in either broadening or narrowing of the distribution. Because of the lack of atomic resolution, we refrain from drawing conclusions about local fluctuations. However, time-resolved fluorescence anisotropy measurements (Fig. 6 *b*) show that the dansyl fluorophore is quite hindered in its motion below 50°C, suggesting limited local flexibility. Details about this will be published separately.

Studying the time-resolved fluorescence of the labeled four-helix bundle $(KE2\text{-}D15)_2$ reveals an interesting heterogeneity of the environment experienced by the dansyl. Only by using time-resolved methods can we obtain information about the distribution of conformations, the width of which we correlate with molecular environments with different degrees of hydration. In an ensemble of four-helix bundle peptides, the observation of a conformational group with a water-containing hydrophobic core (second group of lifetimes) and another group of conformations with a dehydrated hydrophobic core (third group of lifetimes) shows that the structural dynamics corresponds to fluctuations in the four-helix bundle tertiary structure (interhelical interactions), and that somehow water is involved in these conformational transitions.

As noted above, the peak fluorescence lifetimes of the second and third groups (9.9 ns and 20.2 ns, respectively) reveal the presence of one partially hydrated state and one dehydrated state (50). The formation of the partially hydrated state is probably caused by water taking part in the hydrophobic interhelical interactions of the four-helix bundle

(52). This polypeptide structure, with ordered secondary structure elements but disordered tertiary structure, corresponds to a molten globule-like structure (53,54).

Four-helix bundle conformational transitions below 31°C

The pattern of the fluorescence lifetime distributions (Fig. 3 *a*) of dansyl in the four-helix bundle changes abruptly at 31°C. In the following, we will discuss the region in which the emission wavelength is constant (8.9–23°C). Because of the strong and blue-shifted steady-state emission maximum (567 nm; Fig. 6 *a*) and the strongly negative CD, we infer that the whole ensemble of molecules has, on average, a four-helix bundle structure. The nearly bimodal distribution of fluorescence lifetimes shows that the ensemble of four-helix bundles is split, as mentioned above, into two major conformational groups that differ primarily in the hydration of the hydrophobic core.

As noted above, at room temperature and below, we also observe a quenched, ≈4 ns fraction that we tentatively assign to a well-packed structure that is spectroscopically different from the ≈20 ns group. Thus, in this temperature range we observe three conformational subgroups, with the overwhelming majority of the peptide being in either of the two long-lifetime subgroups (see Table 1). If, as we suggest, the ≈4 ns lifetime is due to electron transfer, the actual structural difference between the ≈20 ns subgroup and the ≈4 ns subgroup can be quite small. In the following discussion, we will be concerned with the long-lifetime groups only.

The presence of two major, distinct fluorescence lifetime groups implies that each four-helix bundle assembly changes hydration state on a slower timescale than the lifetime of the fluorescence (tens of nanoseconds). From a protein-folding standpoint, this dynamical equilibrium between the two hydration states corresponds to structural transitions between the four-helix bundle's native (*N*) and molten globule state (*I*), where the molten-globule-like state is characterized by hydrated tertiary interactions. Such compact, native-like, water-containing and transient structures have been observed in simulations of the folding of different proteins, in which the water in the hydrated transient structure was expelled before the native fold was reached (14,55). According to theory, the interaction of hydrophobic solutes with each other proceeds via a solvent-separated state (14,56), where one layer of water molecules separates the hydrophobic parts.

The molten-globule-like fraction accounts for ~60% of the total ensemble of four-helix bundles at room temperature, compared with ~40% at 8.9°C. Increased temperature shifts the conformational equilibrium toward the molten-globule state.

Four-helix bundle conformational transitions above 31°C—opening and closing

Compared with the shape of the distribution at room temperature, the shape of the distribution of fluorescence lifetimes changes significantly as the temperature reaches 31°C. The 4.2 ns peak disappears, and the maximum probable lifetimes of the second and third groups shift from ≈10 ns to ≈7 ns, and from ≈20 ns to ≈16 ns (Table 1), respectively. The coalescence of the fluorescence lifetime distribution into only two separate subdistributions (which we still call the second and third groups) is conserved in the whole temperature region of 31–79°C. Of interest, the peak lifetimes of the second and third groups do not vary significantly with temperature in the interval of 31–60°C, and the only transition that occurs is a redistribution of molecules from the third to the second group (which increases from 27% to 60% of the total fluorescence lifetime distribution), along with a sharpening of the distribution of the third group.

It is worth pointing out that the onset of the red shift of the steady-state emission occurs around 30°C and thus coincides with the coalescence of the lifetime distribution into two separate peaks. The red shift is also in agreement with the population shift from lifetime group 3 to lifetime group 2, that is, from more-dehydrated to more-hydrated structures. This equilibrium between fully hydrated and partly hydrated hydrophobic parts of the four-helix bundle is compatible with transient openings of the four-helix bundle.

In particular, the conformations of the second group should be highly hydrated, as judged from the 7 ns peak fluorescence lifetime. It cannot be excluded that this represents monomers or loosely associated dimers in which the dansyl is partly shielded from water (see below). Hydration of this group increases further, to some extent, when temperature is increased to 79°C, as demonstrated by the reduction of the peak fluorescence lifetime to 5.7 ns. Given the increased thermal motion at high temperatures, more exposure of the dansyl to water is likely.

CD and fluorescence probe different structural changes

Throughout the whole temperature region of 20–80°C, a gradual loss of helicity is observed, as determined by the mean residue ellipticity at 220 nm. Contrasting the fluorescence, there is no threshold below which the CD is temperature-independent. From this it follows, not surprisingly, that CD and fluorescence monitor different aspects of peptide conformational change. Combining the CD and fluorescence results, we arrive at the following picture: helicity is gradually lost throughout the whole temperature range, but the hydrophobic core (or at least the parts that host the dansyls) remains mostly intact up to ~30°C. Such behavior could tentatively be explained by increasing backbone dynamics that leave the parts and side chains that constitute the hydrophobic core mostly unperturbed. Above this transition temperature, the loss of helicity continues as the backbone dynamics increase, but now the hydrophobic core starts to break up, and the structure gradually shifts from a helix bundle to a molten-globule structure.

Since both the shape and position of the peaks of the fluorescence lifetime distribution change dramatically between 9°C and 80°C, the thermally induced dissociation of the four-helix bundle is clearly occurring in multiple steps. However, in the posttransition region between 30°C and 60°C, the unfolding resembles a two-state process (see above). We assign these two states (which in reality are groups of similar conformations) to structures with different degrees of hydration of the hydrophobic core. As noted above, increasing temperature transfers population from the less-hydrated to the more-hydrated conformation. Since the mean residue ellipticity at 220 nm becomes less negative in this process, the helix content of the more-hydrated structures must be lower than that of the less-hydrated structures. Furthermore, in view of the reduced fluorescence lifetimes of both groups, both can be called molten-globule-like.

Judging from the CD data, steady-state emissions, and fluorescence lifetime distributions, it seems highly unlikely that a significant amount of monomer is present at 23°C and below. Since the longer-lifetime group of ~16 ns, which we attribute to a molten-globule dimer, retains a broad shape up to 60°C but narrows considerably along with a shift to shorter lifetimes at 79°C, we take this as an indication that complete dissociation takes places above ~60°C. At 80°C the overall helical content is reduced by 64% compared to room temperature, but the bimodal fluorescence lifetime distribution still indicates two different populations of the peptide. We would again like to stress the point that fluorescence and CD probe different aspects of peptide conformation, and that particularly in the unstructured monomer the emission reports only the local environment around the dansyl.

CONCLUSIONS

Fluorescence lifetime measurements of dansyl, a part of the hydrophobic core of a four-helix bundle peptide, show that the molecular ensemble of a four-helix bundle is divided into two major structural groups. The two groups of conformations differ in their water content. The conformational transitions of this four-helix bundle peptide are equivalent to a hydration and dehydration of the hydrophobic core, corresponding to transitions between the native state (N) and the molten-globule state (I) of the four-helix bundle, where the molten-globule state is characterized by a hydrated/solvated hydrophobic core.

Increasing the temperature further melts the tertiary structure of the four-helix bundle, as evidenced by an increase in the molten-globule conformations. The helical backbone structure, however, remains to some degree despite the loss of tertiary contacts. Dissociated dimers, i.e., helix-loop-helix conformations, are observed at temperatures above 30°C.

The thermally denatured state at 79°C shows a heterogeneous ensemble of polypeptide structures on the nanosecond timescale.

SUPPORTING MATERIAL

Synthesis of KE2-D15 is available at http://www.biophysj.org/biophysj/supplemental/S0006-3495(09)00977-1.

We thank Professor Lars Baltzer (Uppsala University) for kindly providing the peptide and for fruitful discussions. Miss Beatriz Villaroel-Rodriguez (Uppsala University) measured most of the steady-state emission spectra. Dr. Stanislav Kalinin (Umeå University) provided the TCSPC analysis software.

Financial support from the Swedish Foundation for Strategic Research, the K&A Wallenberg Foundation, and the Ingegerd Bergh Foundation is gratefully acknowledged.

REFERENCES

1. Yang, H., G. B. Luo, P. Karnchanaphanurach, T. M. Louie, I. Rech, et al. 2003. Protein conformational dynamics probed by single-molecule electron transfer. *Science*. 302:262–266.
2. Frauenfelder, H., S. G. Sligar, and P. G. Wolynes. 1991. The energy landscapes and motions of proteins. *Science*. 254:1598–1603.
3. Henzler-Wildman, K. A., M. Lei, V. Thai, S. J. Kerns, M. Karplus, et al. 2007. A hierarchy of timescales in protein dynamics is linked to enzyme catalysis. *Nature*. 450:913–916.
4. Munoz, V. 2007. Conformational dynamics and ensembles in protein folding. *Annu. Rev. Biophys. Biomol. Struct*. 36:395–412.
5. Frauenfelder, H., P. W. Fenimore, G. Chen, and B. H. McMahon. 2006. Protein folding is slaved to solvent motions. *Proc. Natl. Acad. Sci. USA*. 103:15469–15472.
6. Cecconi, C., E. A. Shank, C. Bustamante, and S. Marqusee. 2005. Direct observation of the three-state folding of a single protein molecule. *Science*. 309:2057–2060.
7. Grünberg, R., M. Nilges, and J. Leckner. 2006. Flexibility and conformational entropy in protein-protein binding. *Structure*. 14:683–693.
8. Grünberg, R., J. Leckner, and M. Nilges. 2004. Complementarity of structure ensembles in protein-protein binding. *Structure*. 12:2125–2136.
9. Gu, W., and V. Helms. 2005. Dynamical binding of proline-rich peptides to their recognition domains. *Biochim. Biophys. Acta*. 1754:232–238.
10. Venanzi, M., E. Gatto, G. Bocchinfuso, A. Palleschi, L. Stella, et al. 2006. Peptide folding dynamics: a time-resolved study from the nanosecond to the microsecond time regime. *J. Phys. Chem. B*. 110:22834–22841.
11. Liu, P., X. H. Huang, R. H. Zhou, and B. J. Berne. 2005. Observation of a dewetting transition in the collapse of the melittin tetramer. *Nature*. 437:159–162.
12. Sorin, E. J., Y. M. Rhee, M. R. Shirts, and V. S. Pande. 2006. The solvation interface is a determining factor in peptide conformational preferences. *J. Mol. Biol.* 356:248–256.
13. MacCallum, J. L., M. S. Moghaddam, H. S. Chan, and D. P. Tieleman. 2007. Hydrophobic association of α-helices, steric dewetting, and enthalpic barriers to protein folding. *Proc. Natl. Acad. Sci. USA*. 104:6206–6210.
14. Cheung, M. S., A. E. Garcia, and J. N. Onuchic. 2002. Protein folding mediated by solvation: water expulsion and formation of the hydrophobic core occur after the structural collapse. *Proc. Natl. Acad. Sci. USA*. 99:685–690.
15. Guo, W. H., S. Lampoudi, and J. E. Shea. 2003. Posttransition state desolvation of the hydrophobic core of the src-SH3 protein domain. *Biophys. J*. 85:61–69.
16. Daidone, I., M. B. Ulmschneider, A. Di Nola, A. Amadei, and J. C. Smith. 2007. Dehydration-driven solvent exposure of hydrophobic surfaces as a driving force in peptide folding. *Proc. Natl. Acad. Sci. USA*. 104:15230–15235.
17. Qiu, W. H., L. Y. Zhang, Y. T. Kao, W. Y. Lu, T. P. Li, et al. 2005. Ultrafast hydration dynamics in melittin folding and aggregation: helix

formation and tetramer self-assembly. *J. Phys. Chem. B*. 109:16901–16910.

18. Persson, E., and B. Halle. 2008. Nanosecond to microsecond protein dynamics probed by magnetic relaxation dispersion of buried water molecules. *J. Am. Chem. Soc*. 130:1774–1787.
19. Okamura, H., K. Makino, and Y. Nishimura. 2007. NMR dynamics distinguish between hard and soft hydrophobic cores in the DNA-binding domain of PhoB and demonstrate different roles of the cores in binding to DNA. *J. Mol. Biol*. 367:1093–1117.
20. Werner, J. H., R. Joggerst, R. B. Dyer, and P. M. Goodwin. 2006. A two-dimensional view of the folding energy landscape of cytochrome *c*. *Proc. Natl. Acad. Sci. USA*. 103:11130–11135.
21. Weiss, S. 1999. Fluorescence spectroscopy of single biomolecules. *Science*. 283:1676–1683.
22. Mukhopadhyay, S., R. Krishnan, E. A. Lemke, S. Lindquist, and A. A. Deniz. 2007. A natively unfolded yeast prion monomer adopts an ensemble of collapsed and rapidly fluctuating structures. *Proc. Natl. Acad. Sci. USA*. 104:2649–2654.
23. Doose, S., H. Neuweiler, H. Barsch, and M. Sauer. 2007. Probing polyproline structure and dynamics by photoinduced electron transfer provides evidence for deviations from a regular polyproline type II helix. *Proc. Natl. Acad. Sci. USA*. 104:17400–17405.
24. Sahoo, H., D. Roccatano, A. Hennig, and W. M. Nau. 2007. A 10-angstrom spectroscopic ruler applied to short polyprolines. *J. Am. Chem. Soc*. 129:9762–9772.
25. Finke, J. M., P. A. Jennings, J. C. Lee, J. N. Onuchic, and J. R. Winkler. 2007. Equilibrium unfolding of the poly(glutamic acid)(20) helix. *Biopolymers*. 86:193–211.
26. Majumdar, D. S., I. Smirnova, V. Kasho, E. Nir, X. X. Kong, et al. 2007. Single-molecule FRET reveals sugar-induced conformational dynamics in LacY. *Proc. Natl. Acad. Sci. USA*. 104:12640–12645.
27. Lee, J. C., H. B. Gray, and J. R. Winkler. 2005. Tertiary contact formation in α-synuclein probed by electron transfer. *J. Am. Chem. Soc*. 127:16388–16389.
28. Kuzmenkina, E. V., C. D. Heyes, and G. U. Nienhaus. 2005. Single-molecule Forster resonance energy transfer study of protein dynamics under denaturing conditions. *Proc. Natl. Acad. Sci. USA*. 102:15471–15476.
29. Alcala, J. R., E. Gratton, and F. G. Prendergast. 1987. Fluorescence lifetime distributions in proteins. *Biophys. J*. 51:597–604.
30. Chen, H., E. Rhoades, J. S. Butler, S. N. Loh, and W. W. Webb. 2007. Dynamics of equilibrium structural fluctuations of apomyoglobin measured by fluorescence correlation spectroscopy. *Proc. Natl. Acad. Sci. USA*. 104:10459–10464.
31. Abbruzzetti, S., E. Crema, L. Masino, A. Vecli, C. Viappiani, et al. 2000. Fast events in protein folding: structural volume changes accompanying the early events in the N→I transition of apomyoglobin induced by ultrafast pH jump. *Biophys. J*. 78:405–415.
32. Arai, M., K. Ito, T. Inobe, M. Nakao, K. Maki, et al. 2002. Fast compaction of [α]-lactalbumin during folding studied by stopped-flow x-ray scattering. *J. Mol. Biol*. 321:121–132.
33. Plaxco, K. W., I. S. Millett, D. J. Segel, S. Doniach, and D. Baker. 1999. Chain collapse can occur concomitantly with the rate-limiting step in protein folding. *Nat. Struct. Mol. Biol*. 6:554–556.
34. Vidugiris, G. J. A., and C. A. Royer. 1998. Determination of the volume changes for pressure-induced transitions of apomyoglobin between the native, molten globule, and unfolded states. *Biophys. J*. 75:463–470.
35. Margittai, M., J. Widengren, E. Schweinberger, G. F. Schröder, S. Felekyan, et al. 2003. Single-molecule fluorescence resonance energy transfer reveals a dynamic equilibrium between closed and open conformations of syntaxin 1. *Proc. Natl. Acad. Sci. USA*. 100:15516–15521.
36. Nishiguchi, S., Y. Goto, and S. Takahashi. 2007. Solvation and desolvation dynamics in apomyoglobin folding monitored by time-resolved infrared spectroscopy. *J. Mol. Biol*. 373:491–502.
37. Gulotta, M., R. Gilmanshin, T. C. Buscher, R. H. Callender, and R. B. Dyer. 2001. Core formation in apomyoglobin: probing the upper reaches of the folding energy landscape. *Biochemistry*. 40:5137–5143.
38. Gulotta, M., E. Rogatsky, R. H. Callender, and R. B. Dyer. 2003. Primary folding dynamics of sperm whale apomyoglobin: core formation. *Biophys. J*. 84:1909–1918.
39. Hagen, S. J., and W. A. Eaton. 2000. Two-state expansion and collapse of a polypeptide. *J. Mol. Biol*. 301:1019–1027.
40. Liu, Z. R., and H. S. Chan. 2005. Desolvation is a likely origin of robust enthalpic barriers to protein folding. *J. Mol. Biol*. 349:872–889.
41. Enander, K., G. T. Dolphin, and L. Baltzer. 2004. Designed, functionalized helix-loop-helix motifs that bind human carbonic anhydrase II: a new class of synthetic receptor molecules. *J. Am. Chem. Soc*. 126: 4464–4465.
42. Michael, K., and B. H. H. Gilson. 1986. The dielectric constant of a folded protein. *Biopolymers*. 25:2097–2119.
43. Simonson, T., and D. Perahia. 1995. Internal and interfacial dielectric properties of cytochrome *c* from molecular dynamics in aqueous solution. *Proc. Natl. Acad. Sci. USA*. 92:1082–1086.
44. Olofsson, S., and L. Baltzer. 1996. Structure and dynamics of a designed helix-loop-helix dimer in dilute aqueous trifluoroethanol solution. A strategy for NMR spectroscopic structure determination of molten globules in the rational design of native-like proteins. *Fold. Des*. 1:347–356.
45. Olofsson, S., G. Johansson, and L. Baltzer. 1995. Design, synthesis and solution structure of a helix-loop-helix dimer—a template for the rational design of catalytically active polypeptides. *J. Chem. Soc., Perkin Trans*. 2:2047–2056.
46. Habenicht, A., J. Hjelm, E. Mukhtar, F. Bergstrom, and L. B. Å. Johansson. 2002. Two-photon excitation and time-resolved fluorescence: 1. The proper response function for analysing single-photon counting experiments. *Chem. Phys. Lett*. 354:367–375.
47. Vinogradov, S. A., and D. F. Wilson. 2000. Recursive maximum entropy algorithm and its application to the luminescence lifetime distribution recovery. *Appl. Spectrosc*. 54:849–855.
48. Reference deleted in proof.
49. Reference deleted in proof.
50. Haldar, S., H. Raghuraman, and A. Chattopadhyay. 2008. Monitoring orientation and dynamics of membrane-bound melittin utilizing dansyl fluorescence. *J. Phys. Chem. B*. 112:14075–14082.
51. Raghuraman, H., and A. Chattopadhyay. 2003. Organization and dynamics of melittin in environments of graded hydration: a fluorescence approach. *Langmuir*. 19:10332–10341.
52. Sessions, R. B., G. L. Thomas, and M. J. Parker. 2004. Water as a conformational editor in protein folding. *J. Mol. Biol*. 343:1125–1133.
53. Ptitsyn, O. B. 1995. Molten globule and protein folding. *Adv. Protein Chem*. 47:83–229.
54. Arai, M., K. Kuwajima, and C. R. Matthews. 2000. Role of the molten globule state in protein folding. *Adv. Protein Chem*. 53:209–282.
55. Garcia, A. E., and G. Hummer. 2000. Water penetration and escape in proteins. *Proteins*. 38:261–272.
56. Dill, K. A., and S. Bromberg. 2003. Molecular Driving Forces. Garland Science, New York.